An Investigation of the Bonding in $[Ru_2(O_2CCF_3)_4]$ and $[Ru_2(O_2CCF_3)_4(NO)_2]$†

David L. Clark, Jennifer C. Green,* and Catherine M. Redfern
Inorganic Chemistry Laboratory, South Parks Road, Oxford OX1 3QR

Vapour-phase He I and He II photoelectron (p.e.) spectra have been obtained for $[Ru_2(O_2CCF_3)_4]$ and $[Ru_2(O_2CCF_3)_4(NO)_2]$. Extended-Hückel and Fenske–Hall calculations of the model systems $[Ru_2(O_2CH)_4]$ and $[Ru_2(O_2CH)_4(NO)_2]$ were used to analyse the bonding in these complexes and to interpret the p.e. spectra. The p.e. spectrum of $[Ru_2(O_2CCF_3)_4]$ has been unambiguously assigned but the experimental data do not establish whether the ground-state electron configuration is $\sigma^2\pi^4\delta^2\pi^{*3}\delta^{*1}$ or $\sigma^2\pi^4\delta^2\pi^{*2}\delta^{*2}$. The calculations and p.e. spectra support a ground-state configuration of $\sigma^2\pi^4\delta^2\pi^{*4}\delta^{*2}$ for $[Ru_2(O_2CCF_3)_4(NO)_2]$.

The dinuclear carboxylates $[M_2(O_2CR)_4L_2]$ have been structurally characterised for a wide variety of metals.[1–10] In particular, the $[M_2(O_2CR)_4]$ (M = Cr, Mo, or W) species have been well characterised and detailed studies of their electronic structure have been carried out.[11–18] These early transition-metal carboxylates are now well understood and the metal–metal quadruple bond may be described in terms of the $\sigma^2\pi^4\delta^2$ valence-electron configuration, albeit in some cases with extensive configuration interaction.[14] Photoelectron (p.e.) spectroscopy studies can, in principle, provide the most direct source of experimental information about valence electrons in molecules, and have provided conclusive evidence in support of the existence of $\sigma^2\pi^4\delta^2$ quadruple bonds.[19–22]

For many years $[Ru_2(O_2CR)_4]$ species were unknown and attempts to prepare them by reduction of the $[Ru_2(O_2CR)_4]^+$ core were unsuccessful. Recently the Ru^{II}–Ru^{II} complexes $[Ru_2(O_2CR)_4L_2]$ [R = Me, L = H_2O or thf (tetrahydrofuran); R = Et, L = Me_2CO or thf; R = CF_3, L = thf or NO] have been prepared.[23,24] Spin-restricted SCF-$X\alpha$-SW calculations have been performed on the model compounds $[Ru_2(O_2CH)_4]^+$ and $[Ru_2(O_2CH)_4]$ which give rise to the prediction of ground-state electron configurations of $\sigma^2\pi^4\delta^2\pi^{*2}\delta^{*1}$ and $\sigma^2\pi^4\delta^2\pi^{*3}\delta^{*1}$ respectively.[25]

The later transition metals are interesting since the metal–metal antibonding orbitals are now occupied and p.e. studies of these electron-rich species will further our understanding of the metal–metal interaction. To date five complexes of general formula M_2X_8 with metal–metal bonds which involve occupation of the antibonding orbitals have been studied by p.e. spectroscopy; they are $[M_2(hmp)_4]$ (hmp = the anion of 2-hydroxy-6-methylpyridine, M = Rh[26a] or Ru[26b]), $[Re_2Cl_4(PMe_3)_4]$,[27] and $[Rh_2\{HC(NR)_2\}_2(X_2)_2]$ [X_2 = $HC(NR)_2^-$ and $CF_3CO_2^-$].[28] The p.e. studies of the rhodium dimers are consistent with the electron configuration of $\sigma^2\pi^4\delta^2\pi^{*4}\delta^{*2}$ predicted for $[Rh_2(O_2CH)_4]$ by spin-restricted SCF-$X\alpha$-SW calculations,[25] and consequently the presence of a metal–metal single bond. The rhenium species has an electron-rich ($\sigma^2\pi^4\delta^2\delta^{*2}$) metal–metal triple bond. The Ru_2^{4+} core has two fewer electrons than the Rh_2^{4+} core such that the π^* and δ^* orbitals will only be partially occupied. This gives rise to several possible ground-state electronic configurations for the Ru_2^{4+} core. Considering only occupation of the antibonding orbitals the three possible valence configurations are π^{*4}, $\pi^{*3}\delta^{*1}$, or $\pi^{*2}\delta^{*2}$. $[Ru_2(hmp)_4]$ shows a $\pi^{*3}\delta^{*1}$ ground state.[26b]

We have carried out a p.e. study on the two complexes $[Ru_2(O_2CCF_3)_4]$ and $[Ru_2(O_2CCF_3)_4(NO)_2]$ to obtain an experimental determination of the electronic configuration. We have performed extended-Hückel and Fenske–Hall calculations on the model complexes $[Ru_2(O_2CH)_4]$ and $[Ru_2(O_2CH)_4(NO)_2]$ to aid interpretation of the spectra and to enable us to make a direct comparison of theoretical results on the two compounds. For $[Ru_2(O_2CH)_4]$ we focus on the metal–metal interaction of the Ru_2^{4+} core. Upon co-ordination of NO the metal–metal interaction will be altered by a bonding interaction with the axial π-acid ligand. The ruthenium species studied are unique in having only partial occupation of both the π^* and δ^* orbitals and provide valuable insight into our understanding of these electron-rich dinuclear compounds. Part of this work has been communicated in a preliminary form.[29]

Experimental and Computational

The original samples of $[Ru_2(O_2CCF_3)_4L_2]$ (L = thf or NO) were supplied by Professor Wilkinson and Dr. Lindsay of Imperial College, London and further samples were prepared by standard literature methods.[24]

The He I and He II p.e. spectra were obtained on a PES Laboratories model 0078 photoelectron spectrometer interfaced with a Research Machines 380Z microprocessor for data collection. The spectrometer consisted of a photon source, an ionisation chamber, and an electron analyser. The photon source was a Helectros Developments Ltd. helium discharge lamp and could generate both He I and He II radiation ($h\nu$ = 21.21 and 40.81 eV respectively). The lamp was also used to heat the samples. The analyser operates by electrostatic deflection of the electrons in a 127° cylindrical sector, across which the potential is varied to scan through the range of electron kinetic energies (k.e.s). The electrons were detected by a Channeltron electron multiplier. Spectra were collected by repeated scans of about 54 s in order to minimise relative intensity changes of the bands due to temperature fluctuations. There was no apparent drift during data collection.

Both complexes were heated in order to obtain a sufficiently high count rate: $[Ru_2(O_2CCF_3)_4(NO)_2]$ sublimed without decomposition at 54 °C, however, $[Ru_2(O_2CCF_3)_4(thf)_2]$ dissociated whilst being heated in the spectrometer, the first spectrum obtained at 80 °C being that of unco-ordinated thf. As the temperature was increased the spectrum of the base-free complex was obtained at 200 °C.

All spectra were calibrated with reference to xenon, nitrogen, and the helium self-ionisation band [apparent ionisation energy (i.e.) = 4.99 eV].

Relative intensities of the low i.e. bands were determined using a curve-fitting program. The areas found were divided by the kinetic energies of the photoelectrons to obtain values corrected for the discrimination of the analyser against slow electrons.

The calculations were performed on the model systems

---

† *Non-S.I. unit employed:* eV = 1.6×10^{-19} J.

Table 1. Bond lengths[24] (Å) used in the calculations

Bond	$[Ru_2(O_2CH)_4]$	$[Ru_2(O_2CH)_4(NO)_2]$
Ru–Ru	2.276	2.532
Ru–O	2.000	2.000
O–C	1.270	1.270
C–H	1.080	1.080
Ru–N		1.815
N–O		1.113

Table 2. Orbital parameters for ruthenium (EHMO calculation)

Orbital	H_{ii}	ζ_1	ζ_2	c_1	c_2
5*s*	−5.41	1.700			
5*p*	−1.25	1.300			
4*d*	−12.05	3.977	1.836	0.647	0.526

Table 3. Vertical i.e.s (eV) for $[Ru_2(O_2CCF_3)_4]$ and $[Ru_2(O_2CCF_3)_4(NO)_2]$

Band	$[Ru_2(O_2CCF_3)_4]$	$[Ru_2(O_2CCF_3)_4(NO)_2]$
a	8.49	8.61
b	9.00	9.57
c	9.66	9.88
d	10.41	10.49
C_1	12.57	12.58
C_2	13.56	13.41
D	15.90	15.98
E	17.25	17.20
F	18.63	

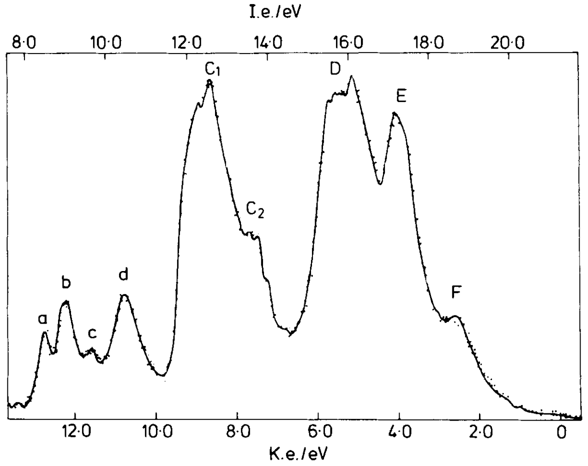

Figure 1. The He I p.e. spectrum of $[Ru_2(O_2CCF_3)_4]$. The counts given refer to the spectrum maximum

$[Ru_2(O_2CH)_4]$ and $[Ru_2(O_2CH)_4(NO)_2]$ using the extended-Hückel molecular orbital[30] (EHMO) and Fenske–Hall[31] computational methods. The co-ordinates were idealised to D_{4h} symmetry but otherwise bond lengths were taken from the crystal structures of $[Ru_2(O_2CCF_3)_4L_2]$ (L = thf or NO).[24] The structural parameters employed in this study are collected in Table 1.

Fenske–Hall calculations were performed using the approximate, non-empirical linear combination of atomic orbitals (l.c.a.o.) procedure of Fenske and Hall which has been described elsewhere.[31] Calculations were performed on an atomic basis for the model compounds $[Ru_2(O_2CH)_4]$ and $[Ru_2(O_2CH)_4(NO)_2]$. Following convergence the results for $[Ru_2(O_2CH)_4(NO)_2]$ were transformed into a basis consisting of the canonical orbitals of the $Ru_2(O_2CH)_4$ and $(NO)_2$ fragments.

Slater atomic orbitals were obtained by optimal fitting of the numerical Herman–Skillman radial functions[32] with Slater-type orbitals. Double-zeta functions were constructed for Ru 4*d* as well as C, O, and N 2*p* atomic orbitals, while single-zeta functions were used for all other orbitals. Valence atomic orbitals (a.o.s) were orthogonalised to all other valence and core orbitals on the same atom. Basis functions for the ruthenium atom were derived for a self-consistent (*via* Fenske–Hall calculation) 0.6+ oxidation state, with the 5*s* and 5*p* exponents fixed at 1.7 and 1.3 respectively. Basis functions for all other atoms were derived for neutral species. An exponent of 1.16 was used for the hydrogen 1*s* atomic orbital.[33]

Extended-Hückel calculations were performed using a modified extended-Hückel method, employing weighted H_{ij} values.[30] The parameters for C, H, N, and O were taken from previous work.[34] The parameters for the Ru atoms were taken from the atomic wavefunction generated for the Fenske–Hall calculation. Only the valence 4*d*, 5*s*, and 5*p* orbitals were used and these parameters are listed in Table 2.

Results and Discussion

Photoelectron Spectra.—The He I and He II p.e. spectra of the two complexes are shown in Figures 1 and 2. The counts given in the figures refer to the maximum counts of the spectrum. The vertical ionisation energies and relative band intensities are collected in Tables 3 and 4.

The spectra can be divided into two main regions. The bands with i.e. > 11 eV are identical for both complexes and Figure 1 shows the full-range He I spectrum of $[Ru_2(O_2CCF_3)_4]$ with band labellings. These bands can be assigned to trifluoroacetate-based ionisations by comparison with the p.e. spectra of the free acid[35] and other $[M_2(O_2CCF_3)_4]$ complexes (M = Cr, Mo, or W).[19–22]

The changes in relative intensity of the low i.e. bands (i.e. < 11 eV) with respect to band C on changing the ionising radiation from He I to He II are consistent with these bands being associated with metal-based levels. Figure 2 shows He I and He II spectra of the metal ionisation region for both complexes. Figure 2(*b*), which is the He II spectrum of $[Ru_2(O_2CCF_3)_4]$, seems to show an extra ionisation feature (with an apparent i.e. between 7.3 and 8 eV and a k.e. of between 32.8 and 33.5 eV) which is not present in the He I spectrum. This is the He IIβ shadow of band D which we would expect to have a k.e. of 32.8 eV.

Further Assignment of P.E. Spectra.—In the metal regions (i.e. < 11 eV) of the spectra (Figure 2) of both complexes four bands, a—d, are evident, whereas ionisations are expected from five orbitals in the metal–metal bonding manifold (σ, π, δ, δ*, and π*). In the case of $[Ru_2(O_2CCF_3)_4]$, where the complex is high spin,[24] more than five bands might be expected, as coupling of the two unpaired electrons to the hole formed on ionisation of a closed shell gives rise to quartet and doublet states. For second-row transition metals, exchange splitting is small, so it is unlikely that the doublet and quartet states are resolved. Therefore the ionisation processes are discussed in terms of the orbital from which an electron is removed, rather than the full symmetry of the ion states formed.

In assigning the five ionisation processes to the four bands we

Table 4. Relative band intensities for the metal-based ionisations of $[Ru_2(O_2CCF_3)_4]$ and $[Ru_2(O_2CCF_3)_4(NO)_2]$ and intensities expected based on electronic degeneracy

Compound	Band	He I	He II[a]	He II/He I	$\pi^{*3}\delta^{*1}$	$\delta^{*2}\pi^{*2}$
$[Ru_2(O_2CCF_3)_4]$	a	1.00	1.00	1.00	1.00	1.00
	b	2.37	2.01	0.85	3.00	1.00
	c	0.85	1.08	1.27	2.00	1.00
	d	4.79	2.24	0.47	6.00	3.00
$[Ru_2(O_2CCF_3)_4(NO)_2]$	a	1.00	1.00	1.00		
	(b + c)	3.17	2.31	0.73		
	d	2.17	1.00	0.46		

[a] The He II band intensities are corrected for the He IIβ shadow of bands D and E.

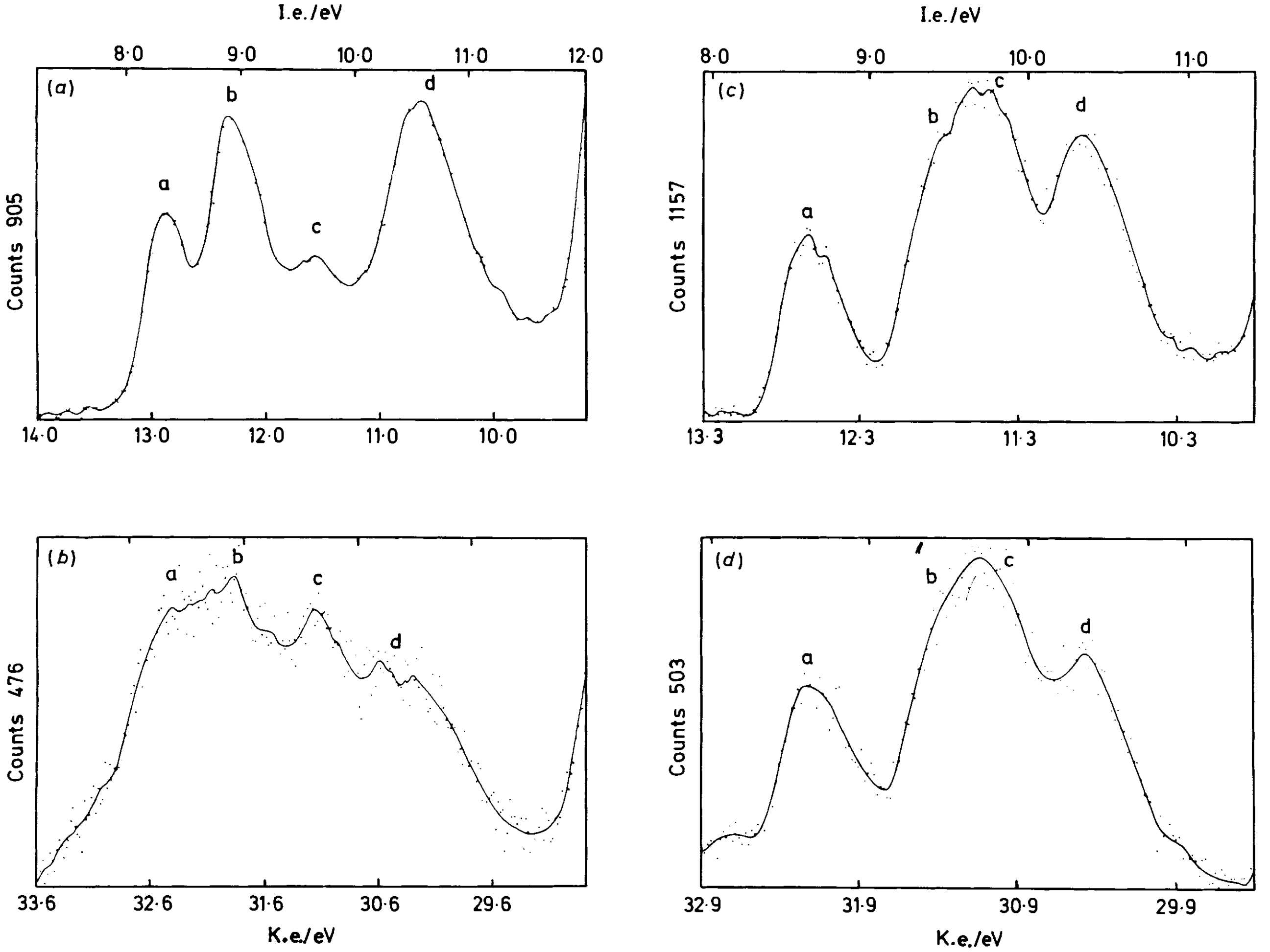

Figure 2. Photoelectron spectra of: (*a*) $[Ru_2(O_2CCF_3)_4]$ (He I), (*b*) $[Ru_2(O_2CCF_3)_4]$ (He II), (*c*) $[Ru_2(O_2CCF_3)_4(NO)_2]$ (He I), and (*d*) $[Ru_2(O_2CCF_3)_4(NO)_2]$ (He II). The counts given refer to the maximum in each spectrum

have various guidelines: (1) comparison of i.e.s with those of related compounds; (2) intensities of bands and their variation with photon energy; (3) information from the calculations (see below). Before proceeding to the assignments, it is helpful to make some points about the nature of the evidence provided by (2).

It is well known that p.e. band intensities in large heteronuclear molecules do not simply follow the degeneracies of the orbitals from which the ionisations take place. They depend, *inter alia*, on the contributions of the different atoms to the m.o.s in question, and they vary differentially with the energy of the exciting radiation.[36] For the $[Mo_2(O_2CCF_3)_4]$ systems the $(\pi + \sigma):\delta$ ratio goes from 5:1 to 2.5:1 (R = H) and from 3:1 to 1.7:1 ($R = CF_3$) when the ionising radiation is changed from He I to He II.[19a] Recent studies using synchrotron radiation to excite the p.e. spectrum of $[Mo_2(O_2CCF_3)_4]$[37] show that the cross-section of the M–M $(\pi + \sigma)$ band decreases by a factor of two when the exciting radiation is changed from 21 (He I) to 42 eV (He *II*), whereas that of the M–M δ band is unaffected. If these results can be extrapolated to the ruthenium compounds studied here, we might expect the δ and δ* orbital bands to gain in intensity relative to π, π*, and σ bands when the ionising radiation is changed from He I to He II.

$[Ru_2(O_2CCF_3)_4]$. It seems reasonable that bands from the σ, π, and δ orbitals should lie at higher i.e.s than those from the π* and δ* orbitals. The (σ + π) band of $[Mo_2(O_2CCF_3)_4]$ has a vertical i.e. of 10.44 eV.[19a] We propose that band d in the p.e. spectrum of $[Ru_2(O_2CCF_3)_4]$, with an i.e. of 10.41 eV, is assigned to a combination of the σ and π ionisations. We assign band c at 9.66 eV to the δ ionisation. The comparable band in $[Mo_2(O_2CCF_3)_4]$ has an i.e. of 8.67 eV, giving a binding energy increase of 1 eV on changing the metal from molybdenum to ruthenium. This is a reasonable shift for an increase in nuclear charge of two. What is more surprising is the insensitivity of the i.e. of the (σ + π) band to the change in metal. This may be due to the higher carboxylate character of the latter orbitals as indicated by the calculation (see below). A similar explanation may be given for the intensity changes between bands c and d (see Table 4). As found for the molybdenum carboxylates, the δ band increases in intensity relative to the (σ + π) band as the ionising radiation is changed from He I to He II; the orbital with the higher *d* character showing a smaller decrease in cross-section in the He II spectrum.

The subsequent assignment of bands a and b to the δ* and π* ionisations is more problematic since it is uncertain whether the ground-state configuration is $\pi^{*3}\delta^{*1}$ or $\delta^{*2}\pi^{*2}$. The restricted Hartree–Fock calculations reported previously[29] predict a ground state of $\sigma^2\pi^4\delta^2\pi^{*2}\delta^{*2}$ for $[Ru_2(O_2CH)_4]$ (as do the EHMO and Fenske–Hall calculations, with the $\sigma^2\pi^4\delta^2\pi^{*3}\delta^{*1}$ state lying 0.65 eV higher in energy. This is in contrast with the earlier results from spin-restricted SCF-$X\alpha$-SW calculations[25] which predict a ground-state configuration of $\sigma^2\pi^4\delta^2\pi^{*3}\delta^{*1}$. At the temperature at which the p.e. spectrum of $[Ru_2(O_2CCF_3)_4]$ was recorded $kT = 0.04$ eV. For the calculated energy gap of 0.65 eV[29] between the two ground states the population of the upper level would be $8.8 \times 10^{-6}\%$. For a 10% population of the upper state the energy gap between the states would have to be 0.09 eV. Therefore it is possible that the p.e. spectrum of $[Ru_2(O_2CCF_3)_4]$ arises from a thermal equilibrium between the two possible ground states. The following assignment of bands a and b is consistent with both possible ground states. On balance we feel the intensity data favour the $\pi^{*3}\delta^{*1}$ configuration with band a assigned to ionisation of the δ* orbital and band b to the π* orbital. This is based partly on the He I relative intensities and also on the higher He II:He I ratio for band a. One problem with this assignment is that the δ and δ* bands are roughly equal in intensity in spite of the difference in their occupancy. However in the Rh_2^{4+} species ($\sigma^2\pi^4\delta^2\pi^{*4}\delta^{*2}$) studies by p.e.s.[26a,28] the band assigned to ionisation from the δ orbital is weaker than the δ* band for equal occupancies, providing support for the above assignment.

Further support for assignment of band a to the δ* ionisation comes from consideration of the spectrum of $[Ru_2(O_2CCF_3)_4(NO)_2]$ discussed below.

$[Ru_2(O_2CCF_3)_4(NO)_2]$. Since NO binds as a σ donor and π acceptor, to first order it will perturb the metal π–π* levels but not the δ–δ* i.e.s. The relative intensity ratio of (a + b + c + d):(C_1 + C_2) for this complex is consistent with there being more electrons in the M–M bonding manifold than for $[Ru_2(O_2CCF_3)_4]$. The first band at 8.61 eV can be assigned to ionisation from the δ* orbital since it has a similar intensity and i.e. to that of the δ* ionisation of $[Ru_2(O_2CCF_3)_4]$. Band d with an i.e. of 10.49 eV is similar to band d in $[Ru_2(O_2CCF_3)_4]$ which suggests assignment of this band to ionisation from the π + σ orbitals. The interaction of the M–M π (e_u) levels with the NO π* e_u combination is expected to be much weaker than the M–M π* (e_g)/NO π* e_g interaction based on the extended-Hückel and Fenske–Hall results (see below). From the calculation this is due to the larger energy gap and smaller degree of overlap for M–M π/NO π* than for M–M π*/NO π*. The second band, b + c, has an i.e. of 9.75 eV and is assigned to ionisation from the π* + δ orbitals. The π* orbital has been stabilised by back bonding to the NO ligand so its i.e. increases relative to $[Ru_2(O_2CCF_3)_4]$, as expected on the basis of the calculations. As the δ orbital cannot interact with the NO ligand its i.e. should be essentially unaltered and thus the δ ionisation must lie under the π* ionisation. This would put the δ ionisation at about the same energy as in $[Ru_2(O_2CCF_3)_4]$. We consider that the similarity in i.e. of bands a and c for the two complexes reinforces the assignments made for $[Ru_2(O_2CCF_3)_4]$.

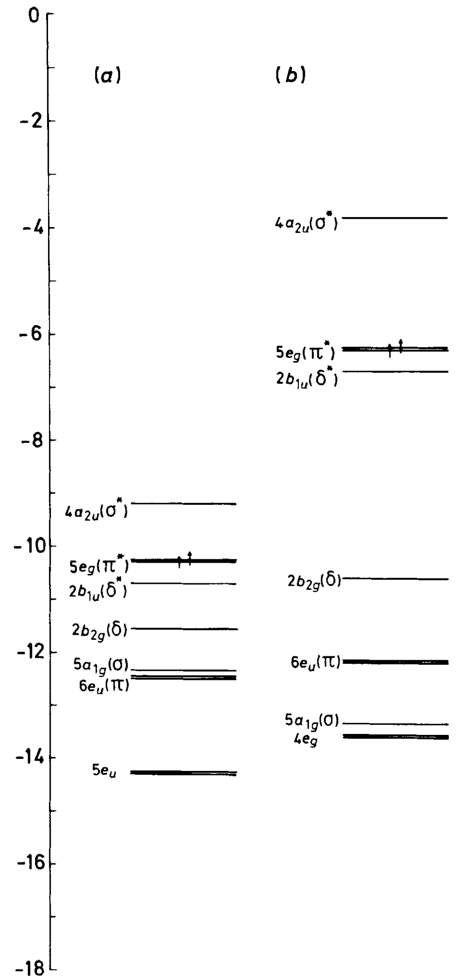

Figure 3. Calculated m.o. diagrams for $[Ru_2(O_2CH)_4]$: (*a*) from extended-Hückel results; (*b*) from Fenske–Hall results

As both calculations (see below) show a large destabilisation of the σ orbital of the metal dimer upon co-ordination of the axial NO ligands, an alternative assignment for the p.e. spectrum of $[Ru_2(O_2CCF_3)_4(NO)_2]$ should be considered. In this, band a is assigned to ionisation of the (σ + δ*) orbitals, bands b + c to the (π* + δ) orbitals, and band d to ionisation from the π orbitals. This assignment is also supported by the ΔSCF calculations reported in our preliminary communication.[29] These predict i.e.s of 7.5 and 7.9 eV for the σ and δ* orbitals respectively. Unfortunately, the relative intensities of the bands, as might be expected from the work discussed above,[37] do not confirm the assignment either way (see Table 4). The He I intensities are closer to the 1:3:3 ratio expected for a

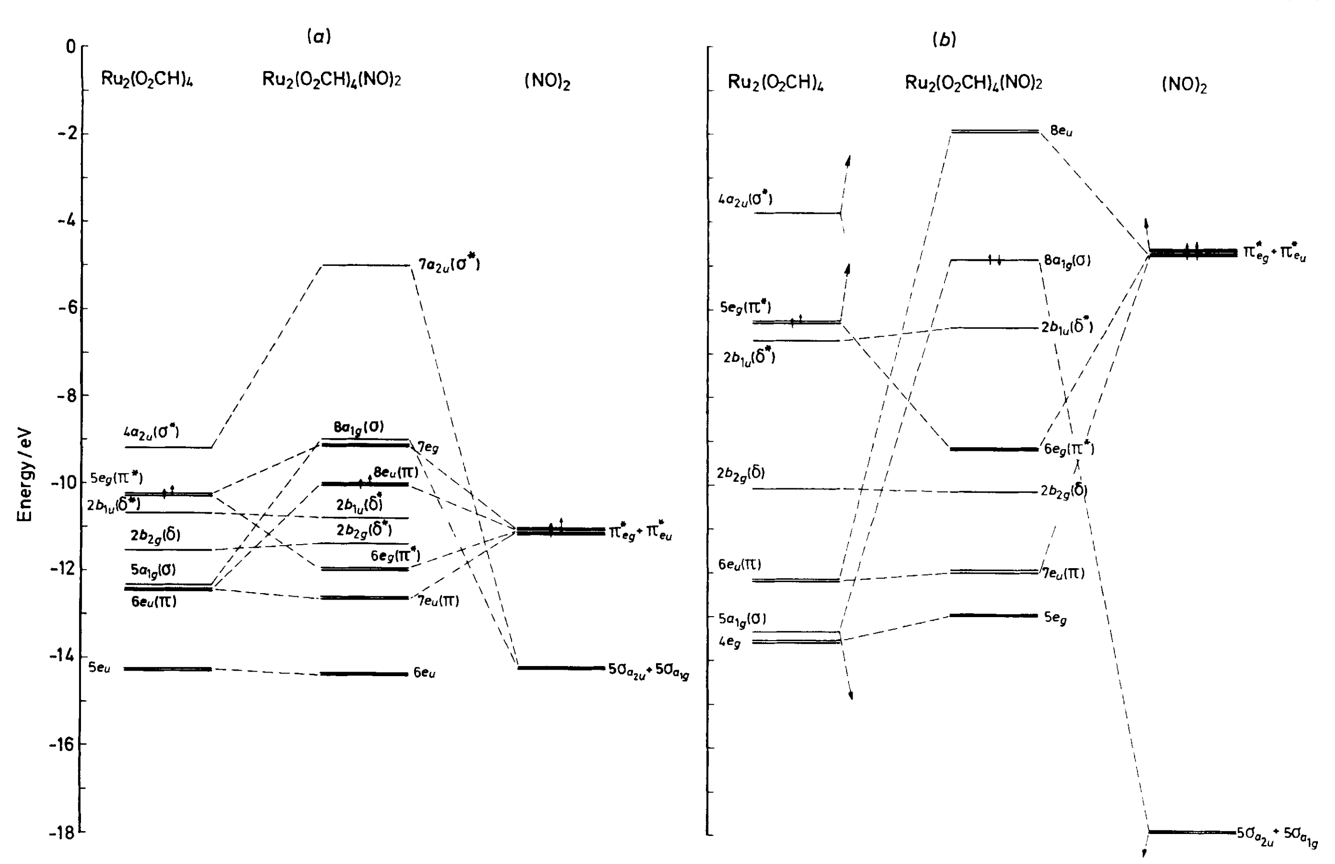

Figure 4. M.o. interaction scheme for $[Ru_2(O_2CH)_4(NO)_2]$: (*a*) from extended-Hückel results; (*b*) from Fenske–Hall results

$(\delta^{*2})(\pi^{*4}\delta^2)(\pi^4\sigma^2)$ assignment, but the He II ratios tend towards 2 : 3 : 2 which would be expected for a $(\delta^{*2}\sigma^2)(\pi^{*4}\delta^2)(\pi^4)$ assignment. The He II–He I intensity ratios (Table 4) of bands a and d in the two complexes are the same indicating a similar assignment in both cases. The weight of evidence from the calculations seems to indicate the $(\delta^{*2}\sigma^2)(\pi^{*4}\delta^2)(\pi^4)$ assignment. The strongest argument against this assignment is the large energy difference (6.15 eV from p.e.s) between the NO 5σ orbitals and the metal–metal σ orbital, which would imply that the M–NO σ interaction would be weak.

Calculations on $[Ru_2(O_2CH)_4]$.—Though the computational methods used are not sufficiently sophisticated to predict accurate ionisation data, they should prove useful in two ways. First, they should give an indication of likely ground-state configurations for the molecules in question. Secondly, changes in orbital energy between $[Ru_2(O_2CH)_4]$ and $[Ru_2(O_2CH)_4(NO)_2]$ would be expected to be similar to the changes in i.e. between related bands in the p.e. spectra.

All valence orbitals were treated in the calculations. Since our interest lies in the assignment and interpretation of the metal-based ionisations, the following discussion is limited to orbitals in the M–M bonding manifold.

For $[Ru_2(O_2CH)_4]$ there are 12 electrons associated with metal–metal bonding. The EHMO calculation gives an electron configuration of $\pi^4\sigma^2\delta^2\delta^{*2}\pi^{*2}$ (σ/π separation only 0.03 eV) and the Fenske–Hall calculation gives $\sigma^2\pi^4\delta^2\delta^{*2}\pi^{*2}$, the m.o. diagrams are given in Figure 3. These orbital orderings are in agreement with calculations on the $[Mo_2(O_2CH)_4]$ system[11–18] and the restricted Hartree–Fock calculations carried out on $[Ru_2(O_2CH)_4]$.[29] Spin-restricted SCF-*X*α-SW calculations have been performed on $[Ru_2(O_2CH)_4]$[25] and these give an orbital energy ordering of $\pi^* < \delta^*$, and consequently an electron configuration $\sigma^2\pi^4\delta^2\pi^{*3}\delta^{*1}$. The high-spin configuration is favoured by close spacing of the π* and δ* orbitals. More recently, magnetic measurements have been made on the series $[Ru_2(O_2CR)_4L_2]$ (R = Me, L = H_2O or thf; R = Et, L = Me_2CO or thf; R = CF_3, L = thf),[23,24] and the observed $\mu_{eff.}$ of 2—2.2 per ruthenium is consistent with two unpaired electrons per binuclear unit. The reversal of the π*/δ* ordering has been rationalised by (1) a downward shift of metal 4*d* levels relative to ligand levels from Mo to Ru to Rh, and (2) the influence of the carboxylate ligands on metal-based orbitals.[25] Both the EHMO and Fenske–Hall calculations bring the π* orbital very close in energy to the δ* orbital (splittings are 0.41 and 0.45 eV respectively).

The Fenske–Hall calculation allows for an easy breakdown of the molecular orbitals into per cent atomic orbital character. From this we see that the π* orbital is about 90% metal localised, 70% δ*, 80% δ, 60% π, and 58% σ, so there are significant carboxylate contributions to these predominantly metal-based orbitals.

Calculation on $(NO)_2$.—Calculations were performed on the free ligand to facilitate a direct comparison of the nitrosyl ligand before and after co-ordination to the metal carboxylate. The geometry used placed the NO molecules at the positions they would occupy in the $[Ru_2(O_2CH)_4(NO)_2]$ complex.

The main differences between the two theoretical techniques were the energy gap between the NO 5σ and π* orbitals and their position relative to the orbitals of $[Ru_2(O_2CH)_4]$ (Figure 4). The Fenske–Hall method gives a 5σ/π* gap of 12.75 eV while the extended-Hückel method gives 3.12 eV. These computed orbital-energy differences can be compared with a value of 7 eV

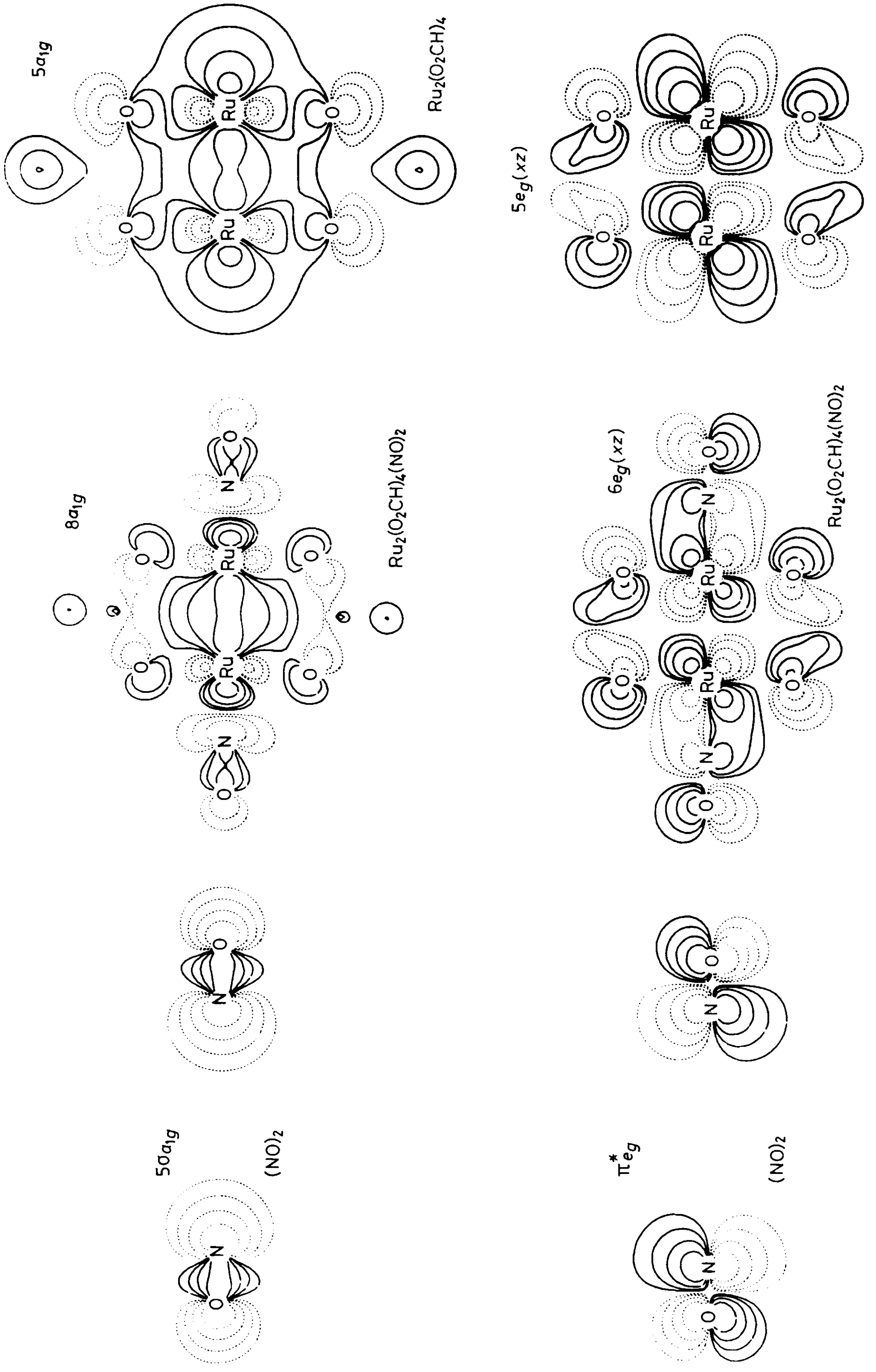

Figure 5. Contour plots of the $Ru_2(O_2CH)_4$ $5a_{1g}$ and $5e_g$ orbitals and the $(NO)_2$ $5\sigma(a_{1g})$ and $\pi^*(e_g)$ orbitals showing their combination to give the $8a_{1g}$ and $6e_g$ orbitals of $[Ru_2(O_2CH)_4(NO)_2]$

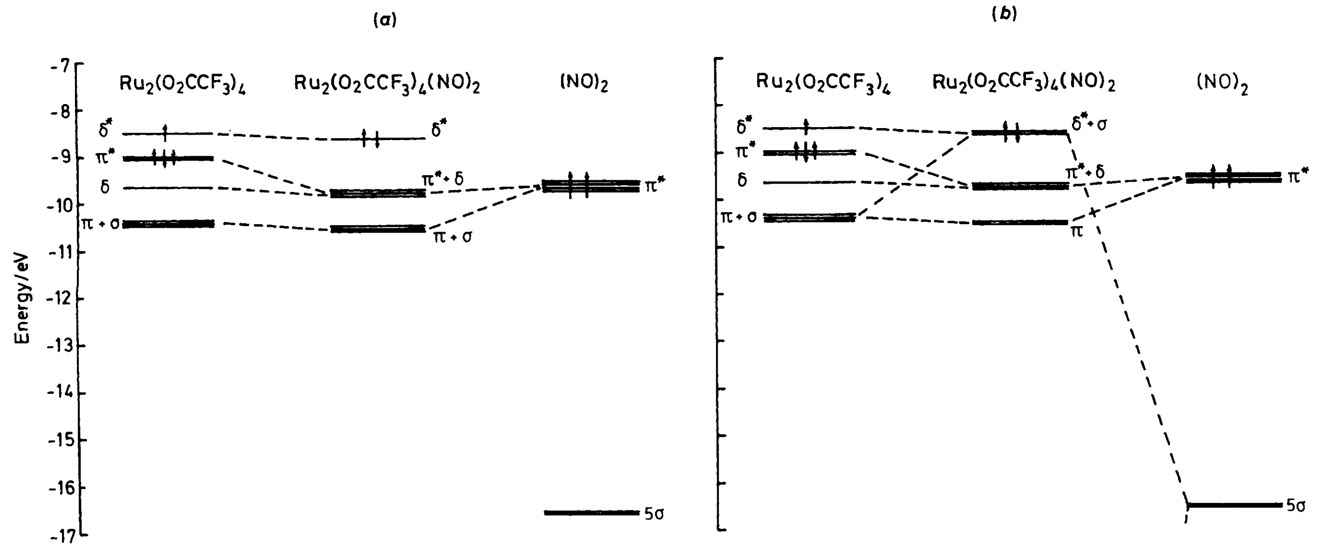

Figure 6. Reverse Koopmans interaction scheme for $[Ru_2(O_2CCF_3)_4(NO)_2]$ based on the two assignments

from the difference of the first two i.e.s of NO (9.54 and 16.56 eV);[38] these results serve to indicate how inadequate the combination of Koopmans' theorem and either computational method is in predicting i.e. patterns (see above).

Calculations of $[Ru_2(O_2CH)_4(NO)_2]$.—Theoretical calculations on a variety of $[M_2(O_2CH)_4]$ and $[M_2(O_2CH)_4L_2]$ compounds have helped to reveal both quantitative and qualitative details of the electronic effects of axial ligation.[11,24,39–41] All of the calculations indicate that the interaction of the $[M_2(O_2CH)_4]$ moiety with an axial ligand is essentially a σ-only interaction. It is found that the M–M π, δ, δ*, π*, and formate orbitals all have nearly identical energies in $[M_2(O_2CH)_4]$ and $[M_2(O_2CH)_4L_2]$. Even for axial ligands containing π lone-pair orbitals, the latter are found to be essentially non-interacting with the $[M_2(O_2CH)_4]$ moiety. The reason for lack of axial-ligand π-lone-pair interaction with metal-based orbitals is that the π lone pairs are energetically too far away and lack sufficient overlap. In the case of the axial NO ligand the partially occupied NO π* orbitals are expected to be energetically much closer and the possibility of π back bonding is introduced. Also, the σ lone-pair orbitals are very much more stable and less likely to perturb the σ system of the M–M bond.

The results of extended-Hückel and Fenske–Hall calculations on $[Ru_2(O_2CH)_4(NO)_2]$ are in accord with the above expectations for the π levels. The correlation of the m.o.s of $[Ru_2(O_2CH)_4(NO)_2]$ with those of its component fragments $Ru_2(O_2CH)_4$ and $(NO)_2$ is shown in Figure 4. As expected from simple group theory, the M–M δ, δ*, M–O, and formate levels in $[Ru_2(O_2CH)_4(NO)_2]$ are essentially unperturbed by interaction of $Ru_2(O_2CH)_4$ with the axial NO ligands.

The axial NO ligand interaction manifests itself as both σ and π interactions with the dinuclear centre. Unlike other axial ligands, for NO a significant π interaction is observed. Symmetric and antisymmetric combinations of NO π* orbitals give rise to e_u and e_g combinations which, by symmetry, can interact with M–M π and π* orbitals respectively. Since the M–M π bond is energetically removed and the overlap is small, it is relatively unperturbed by the axial NO interaction. By contrast, the M–M π* orbital is energetically closer, has better overlap, and is dramatically stabilised by interaction as shown in Figure 4. Thus we arrive at a closed-shell M–M bonding configuration of $\pi^4\delta^2\pi^{*4}\delta^{*2}\sigma^2$ as predicted by restricted Hartree–Fock calculations.[29] These combinations of $Ru_2(O_2CH)_4$ and $(NO)_2$ σ and π* orbitals are shown as contour plots in Figure 5.

The percent atomic character of the $7e_u$ and $6e_g$ molecular orbitals indicates the importance of the M–M π*/NO π* interaction. The $7e_u(\pi)$ orbitals are 46% metal localised and 15% NO localised whereas the $6e_g(\pi^*)$, although also 46% metal localised, are now 28% NO localised. In $[Ru_2(O_2CH)_4]$ the π* orbitals had the greatest metal localisation.

The extended-Hückel results reveal essentially identical interactions between the metal and axial ligand, however the magnitudes of the interaction are altered significantly. Again the M–M π, δ, δ*, M–O, and formate levels are relatively unperturbed, while the e_g M–M π* orbital is stabilised by axial NO-ligand interaction. The major difference is that the a_{1g} σ interaction between the symmetric combination of NO σ lone pairs and the M–M σ bond is so strong that the M–M σ bonding orbital is pushed up and out of the manifold of occupied M–M bonding orbitals. As a result, the e_u combination of NO π* orbitals accommodates these electrons and we arrive at an open-shell electronic configuration of $\pi^4\pi^{*4}\delta^2\delta^{*2}\pi^{*2}$. This cannot be the correct description of the valence electron configuration of $[Ru_2(O_2CCF_3)_4(NO)_2]$ as the complex is diamagnetic.[24] This is shown in the correlation diagram for the extended-Hückel results in Figure 4.

The changes in the M–M σ orbital energy as seen in the comparison of extended-Hückel and Fenske–Hall results is not at all surprising in view of its extreme sensitivity to relatively small changes in M–M and M–L distances as well as sphere radii in $X\alpha$-SW calculations performed by other workers.[13] This places obvious doubts on the actual placement of the M–M σ orbital relative to other orbitals in the M–M bonding manifold. Using the Fenske–Hall method, we have found that a relatively small perturbation in the Ru–N distance generates a relatively large change in the M–M σ orbital energy, while leaving the other orbitals essentially unchanged.

A reverse Koopmans interaction scheme has been constructed from the p.e. data on the two complexes for both assignments given above for $[Ru_2(O_2CCF_3)_4(NO)_2]$ (Figure 6). Such a diagram uses the negative of the i.e.s of the bands in a p.e. spectrum as the orbital energies for the complex. This can be compared with the correlation diagrams from the calculations (Figure 4). The main difference between the theoretical models and the reverse Koopmans scheme is the magnitude of the interaction of the NO π^* and σ orbitals with the metal levels, and the consequent placement of the σ orbital.

In conclusion, the present analysis of the u.v.–p.e. data and molecular-orbital calculations on $[Ru_2(O_2CCF_3)_4]$ and $[Ru_2(O_2CCF_3)_4(NO)_2]$ leads to an unambiguous assignment of the p.e. spectrum of $[Ru_2(O_2CCF_3)_4]$. However, the experimental data do not establish whether the ground state is $\sigma^2\pi^4\delta^2\pi^{*3}\delta^{*1}$, as predicted by spin-restricted SCF-$X\alpha$-SW calculations,[25] or $\sigma^2\pi^4\delta^2\pi^{*2}\delta^{*2}$, as predicted by restricted Hartree–Fock calculations.[29]

For $[Ru_2(O_2CCF_3)_4(NO)_2]$ a ground-state electron configuration of $\sigma^2\pi^4\delta^2\pi^{*4}\delta^{*2}$ is supported by both the experimental and theoretical data. The experimental evidence cannot distinguish conclusively between the $(\delta^{*2}\sigma^2)(\pi^{*4}\delta^2)(\pi^4)$ and $(\delta^{*2})(\pi^{*4}\delta^2)(\pi^4\sigma^2)$ assignments for the bis(nitrosyl) adduct, but the results of the calculations favour the $(\delta^{*2}\sigma^2)(\pi^{*4}\delta^2)(\pi^4)$ assignment.

Acknowledgements

We thank Sir G. Wilkinson and Dr. A. J. Lindsay for the original samples, the S.E.R.C. for financial support, and the Dee Corporation for a scholarship (to C. M. R.).

References

1 G. C. Aleksandrov and Y. T. Struchkov, *J. Organomet. Chem.*, 1971, **27**, 53; *J. Struct. Chem.*, 1970, **11**, 438.

2 F. A. Cotton, M. W. Extine, and G. W. Rice, *Inorg. Chem.*, 1978, **17**, 176; F. A. Cotton and G. W. Rice, *Inorg. Chem.*, 1978, **17**, 688, 2004 and refs. therein.

3 R. J. Doedens, *Prog. Inorg. Chem.*, 1976, **21**, 209.

4 J. Drew, M. B. Hursthouse, P. Thornton, and A. S. Welch, *J. Chem. Soc., Chem. Commun.*, 1978, 52.

5 F. A. Cotton, M. W. Extine, and L. D. Gage, *Inorg. Chem.*, 1978, **17**, 172 and refs. therein.

6 F. A. Cotton and L. D. Gage, *Nouv. J. Chim.*, 1977, **1**, 441.

7 M. J. Bennett, K. G. Caulton, and F. A. Cotton, *Inorg. Chem.*, 1969, **8**, 1.

8 F. A. Cotton, B. G. DeBoer, M. D. LaPrade, J. R. Pipal, and P. A. Ucko, *Acta Crystallogr., Sect. B*, 1971, **27**, 1664; G. G. Cristoph and Y.-B. Koh, *J. Am. Chem. Soc.*, 1979, **101**, 1422; J. J. Zrowlski, M. Mosziar, and T. Glowiak, *J. Chem. Soc., Chem. Commun.*, 1977, 760.

9 M. J. Bennett, W. K. Bratton, F. A. Cotton, and W. R. Robinson, *Inorg. Chem.*, 1970, **2**, 1570.

10 A. P. Sattelberger, K. W. McLaughin, and J. C. Huffman, *J. Am. Chem. Soc.*, 1981, **103**, 2880.

11 M. D. Braydich, B. E. Bursten, M. H. Chisholm, and D. L. Clark, *J. Am. Chem. Soc.*, 1985, **107**, 4459.

12 B. E. Bursten and D. L. Clark, *Polyhedron*, 1987, **6**, 695 and refs. therein.

13 J. G. Norman, jun., H. J. Kolari, H. B. Gray, and W. C. Trogler, *Inorg. Chem.*, 1977, **16**, 987.

14 M. Benard, *J. Am. Chem. Soc.*, 1987, **100**, 2354.

15 P. M. Atha, I. H. Hillier, and M. F. Guest, *Mol. Phys.*, 1982, **46**, 437.

16 T. Ziegler, *J. Am. Chem. Soc.*, 1985, **107**, 4453.

17 I. H. Hillier, C. D. Garner, G. R. Mitcheson, and M. F. Guest, *J. Chem. Soc., Chem. Commun.*, 1978, 204.

18 F. A. Cotton and G. G. Stanley, *Inorg. Chem.*, 1977, **16**, 2668.

19 (*a*) A. W. Coleman, J. C. Green, A. J. Hayes, E. A. Seddon, D. R. Lloyd, and Y. Niwa, *J. Chem. Soc., Dalton Trans.*, 1979, 1057; (*b*) J. C. Green and A. J. Hayes, *Chem. Phys. Lett.*, 1975, **31**, 306, (*c*) C. D. Garner, I. H. Hillier, M. F. Guest, J. C. Green, and A. W. Coleman, *Chem. Phys. Lett.*, 1976, **41**, 91; (*d*) F. A. Cotton, J. G. Norman, jun., B. R. Stults, and T. R. Webb, *J. Coord. Chem.*, 1976, **5**, 217.

20 D. L. Lichtenberger and C. H. Blevin II, *J. Am. Chem. Soc.*, 1984, **106**, 1636.

21 E. M. Kobes and D. L. Lichtenberger, *J. Am. Chem. Soc.*, 1985, **107**, 7199.

22 G. M. Bancroft, E. Pellach, A. P. Sattelberger, and K. W. McLaughlin, *J. Chem. Soc., Chem. Commun.*, 1982, 752.

23 A. J. Lindsay, G. Wilkinson, M. Motavelli, and M. B. Hursthouse, *J. Chem. Soc., Dalton Trans.*, 1985, 2321.

24 A. J. Lindsay, G. Wilkinson, M. Motavelli, and M. B. Hursthouse, *J. Chem. Soc., Dalton Trans.*, 1987, 2723.

25 J. G. Norman, jun., G. E. Renzoni, and D. A. Case, *J. Am. Chem. Soc.*, 1979, **101**, 5256.

26 (*a*) M. Berry, C. D. Garner, I. H. Hillier, A. A. MacDowell, and W. Clegg, *J. Chem. Soc., Chem. Commun.*, 1980, 494; (*b*) M. Berry, C. D. Garner, I. H. Hillier, and A. A. MacDowell, *Inorg. Chim. Acta*, 1981, **53**, 161.

27 D. R. Root, C. H. Blevin II, D. L. Lichtenberger, A. P. Sattelberger, and R. A. Walton, *J. Am. Chem. Soc.*, 1986, **108**, 953.

28 G. A. Rizzi, M. Casarin, E. Tondello, P. Piraino, and G. Granozzi, *Inorg. Chem.*, 1987, **26**, 3406.

29 D. L. Clark, J. C. Green, C. M. Redfern, G. E. Quelch, I. H. Hillier, and M. F. Guest, *Chem. Phys. Lett.*, in the press.

30 R. Hoffman and W. N. Lipscomb, *J. Chem. Phys.*, 1962, **36**, 2179.

31 M. B. Hall and R. F. Fenske, *Inorg. Chem.*, 1972, **11**, 768.

32 B. E. Bursten, J. R. Jensen, and R. F. Fenske, *J. Chem. Phys.*, 1978, **68**, 3320.

33 W. J. Hehre, R. F. Stewart, and J. A. Pople, *J. Chem. Phys.*, 1969, **51**, 2657.

34 T. A. Albright, R. Hoffman, J. C. Thibeault, and D. L. Thorn, *J. Am. Chem. Soc.*, 1979, **101**, 3801.

35 E. A. Seddon, D.Phil. Thesis, Oxford, 1980.

36 A. Berndtsson, E. Basilier, U. Gelius, J. Hedman, M. Klasson, R. Nilsson, C. Nording, and S. Svensson, *Phys. Scripta*, 1975, **12**, 235.

37 J. G. Brennan, G. Cooper, J. C. Green, M. P. Payne, and C. M. Redfern, unpublished work.

38 O. Edquist, E. Lindholm, L. E. Selin, H. Ejogren, and L. Asbrink, *Ark. Fysik.*, 1970, **40**, 439.

39 B. E. Bursten and F. A. Cotton, *Inorg. Chem.*, 1981, **20**, 3042.

40 J. G. Norman, jun., and H. J. Kolari, *J. Am. Chem. Soc.*, 1978, **100**, 791.

41 D. L. Lichtenberger and J. G. Kristofzski, *J. Am. Chem. Soc.*, 1987, **109**, 3458.

Received 22nd March 1988; *Paper* 8/01174E